First publ. in: European Journal of Biochemistry 264 (1999), 1, pp. 140-151

Kinetic mechanisms of cholesterol oxidase from *Streptomyces hygroscopicus* and *Brevibacterium sterolicum*

Loredano Pollegioni[1], Gaby Wels[2], Mirella S. Pilone[1] and Sandro Ghisla[2]

[1]*Department of Structural and Functional Biology, University of Insubria, Varese, Italy;* [2]*Faculty of Biology, University of Konstanz, Germany*

The kinetic properties of two cholesterol oxidases, one from *Brevibacterium sterolicum* (BCO) the other from *Streptomyces hygroscopicus* (SCO) were investigated. BCO works via a ping-pong mechanism, whereas the catalytic pathway of SCO is sequential. The turnover numbers at infinite cholesterol and oxygen concentrations are 202 s^{-1} and 105 s^{-1} for SCO and BCO, respectively. The rates of flavin reduction extrapolated to saturating substrate concentration, under anaerobic conditions, are 235 s^{-1} for BCO and 232 s^{-1} for SCO (in the presence of 1% Thesit and 10% 2-propanol). With reduced SCO the rate of Δ5-6→Δ4-5 isomerization of the intermediate 5-cholesten-3-one to final product is slow (0.3 s^{-1}). With oxidized SCO and BCO the rate of isomerization is much faster (≈300 s^{-1}), thus it is not rate-limiting for catalysis. The kinetic behaviour of both reduced COs towards oxygen is unusual in that they exhibit apparent saturation with increasing oxygen concentrations (extrapolated rates ≈250 s^{-1} and 1.3 s^{-1}, for BCO and SCO, respectively): too slow to account for catalysis. For BCO the kinetic data are compatible with a step preceding the reaction with oxygen, involving interconversion of reactive and nonreactive forms of the enzyme. We suggest that the presence of micelles in the reaction medium, due to the necessary presence of detergents to solubilize the substrate, influence the availability or reactivity of oxygen towards the enzyme. The rate of re-oxidation of SCO in the presence of product is also too slow to account for catalysis, probably due to the impossibility of producing quantitatively the reduced enzyme–product complexes.

Keywords: cholesterol oxidase; flavoenzyme; kinetic mechanism; steroid.

Cholesterol oxidase (CO, EC 1.1.3.6) is a flavoprotein that catalyses the dehydrogenation of C(3)-OH of the cholestan system. It is therefore an alcohol dehydrogenase/oxidase belonging to the glucose–methanol–choline (GMC) oxidoreductase family [1]. Oxidized flavin is the primary acceptor of hydride from the alcohol. The reduced flavin then transfers the redox equivalents to dioxygen as final acceptor. CO has been isolated from a variety of organisms, mainly fungi. The three-dimensional structure of the CO from *Brevibacterium* sp., which contains noncovalently linked FAD, has been reported by Vrielink *et al*. [2]. Intriguingly a second cholesterol oxidase from a strain of *Brevibacterium* contains a covalently linked 8-histidyl-FAD. This situation brings to mind the two nicotinic acid oxidases present in *Arthrobacter oxidans,* distinguished not only by differences in FAD-binding [3] but also by the fact that the enzyme linked covalently to FAD is specific for the substrate D-form, and the other acts specifically on the L-form. These considerations prompted us to compare two related COs, one from *Streptomyces hygroscopicus* (SCO) containing noncovalently linked FAD, the other a recombinant protein from *Brevibacterium sterolicum* (BCO) is expressed in *Escherichia coli* and contains covalently linked FAD. The redox and comparative properties of these two enzymes have been described recently [4]. A methodological investigation of the effects of detergents and solvents on the properties of SCO and BCO is given in Pollegioni *et al*. [5] and provides a necessary background to the present study.

CO has received considerable attention because of its use in enzymatic cholesterol analysis [6] and agriculture [7]. Several studies on its catalytic and other properties [8–11] and applications [6,7] have been published. More recently its mechanism received some attention [4] and studies based on directed mutagenesis have appeared [12]. However, no work on the kinetic mechanism of catalysis has appeared so far, undoubtedly due to the difficulties arising from the poor solubility of sterol substrates, which necessitate the use of detergents and preclude studies under well-defined conditions.

We have now performed an investigation of the kinetic properties of these two enzymes, spurred on by the fact that the three-dimensional structure of BCO (covalently bound FAD) [13] is close to completion (A. Vrielink, personal communication). Comparison of the latter with the three-dimensional structure of the CO from *B. sterolicum* [2], particularly in light of the data presented here, will considerably expand our understanding of this class of enzyme.

Correspondence to L. Pollegioni, Department of Structural and Functional Biology, University of Insubria via J.H. Dunant 3, 21100 Varese, Italy.
Fax: +39 033 242 1500, Tel.: + 39 033 242 1506,
E-mail: polleg@imiucca.csi.unimi.it

Abbreviations: androstensulfate, androst-5-en-3β-ol-β-17-sulfate; BCO, recombinant cholesterol oxidase from *Brevibacterium sterolicum* expressed in *E. coli*; cholestanol, 5α-cholestan-3β-ol; cholesterol, 5-cholestene-3β-ol; CO, cholesterol oxidase; EMTN, enzyme-monitored turnover; GMC, glucose–methanol–choline; HRP, horseradish peroxidase; pregesterone, 4-pregnene-3,20-dione; pregnenolone, 5-pregnene-3β-ol-20-one; SCO, cholesterol oxidase from *Streptomyces hygroscopicus*; *trans*-androsterone, 5α-androstan-3β-ol-17-one; *trans*-dehydroandrosterone, 5-androstene-3β-ol-17-one.

Enzymes: cholesterol oxidase (EC 1.1.3.6); horseradish peroxidase (EC 1.11.1.7).

MATERIALS AND METHODS

Materials and enzymes

Cholesterol, *trans*-dehydroandrosterone, *trans*-androsterone, pregnenolone, cholestanol, Thesit® and Triton X-100® were purchased from Boehringer Mannheim. Androstensulphate was a kind gift from Dr D. Edmondson (Emory University, USA). All other reagents were of the highest commercially available purity. SCO, purified from *S. hygroscopicus* cells, and recombinant *B. sterolicum* CO, from *E. coli*, were obtained from Roche Diagnostics.

Enzymatic activity

Cholesterol oxidase activity was assayed at 25 °C using six different methods during the course of the investigations. These are as follows: test 1 measured oxygen consumption polarographically; tests 2 and 3 (Table 1) monitored the production of 4-cholesten-3-one spectrophotometrically at 240 nm (ε_{240} = 15 500 $M^{-1}\cdot cm^{-1}$); tests 4 and 5 monitored H_2O_2 production at 440 nm (ε_{440} = 13 000 $M^{-1}\cdot cm^{-1}$) in enzyme-coupled assays with horseradish peroxidase (HRP) as described in Gadda *et al*. [4]. The last method was the enzyme-monitored turnover (EMTN) method [14] in which enzyme was mixed with substrate in a stopped-flow instrument and the absorption change was monitored at 446 nm and 467 nm (for BCO and SCO, respectively) to follow reaction progress.

Test 4 employed 2 $\mu g\cdot mL^{-1}$ HRP, 4 $mg\cdot mL^{-1}$ of 3,5-dichlorosulphonate and 0.8 $mg\cdot mL^{-1}$ of 4-aminoantipyrine; test 5 employed 10 $\mu g\cdot mL^{-1}$ HRP and 0.16 $mg\cdot mL^{-1}$ *o*-dianisidine. Tests 2 and 4 used 0.5 M potassium phosphate buffer, pH 7.5, containing 0.4% Thesit; tests 3 and 5 were in 100 mM phosphate buffer, pH 7.5, containing 0.2% Thesit; test 1 was carried out at both these potassium phosphate concentrations.

Absorption and fluorescence measurements

UV-visible absorption spectra were recorded with an Uvikon 930 spectrophotometer (Kontron Instr.) in potassium phosphate buffer, pH 7.5, 25 °C.

Determination of critical micelle concentration

The critical micelle concentrations of cholesterol, 5-cholesten-3-one and 4-cholesten-3-one were estimated at 25 °C in 50 mM potassium phosphate buffer, pH 7.5, using a dye-binding technique with 24 μM rhodamine 6G as indicator and following the absorbance change at 525 nm [15].

Rapid reaction (stopped-flow) measurements

Rapid reaction measurements and turnover experiments were carried out at 25 °C in 50 mM potassium phosphate buffer, pH 7.5, in the presence of various concentrations of Thesit (0–10%) and 2-propanol (0–10%), in a thermostated stopped-flow spectrophotometer, with a cell path length of 2 cm. The diode array detector of this instrument was interfaced with a Macintosh IIcx computer and the program POSMA was used for data acquisition and manipulation (Spectroscopy Instruments GmbH Gilching, Germany; [16]). All concentrations mentioned in these experiments are those after mixing, i.e. at 1 : 1 dilution. Rapid reactions were routinely recorded in the 300–650 nm wavelength range using the normal scan mode (scan time 10 ms per spectrum, resolution of 2 $pixel\cdot nm^{-1}$). For fast reactions ($k_{obs} \geq 50\ s^{-1}$) a 'fast access' routine was used, with an acquisition time of ≈1 ms per spectrum and a resolution of 5 nm. For re-oxidation experiments, the enzyme was first reduced with a 1.5-fold excess of substrate under anaerobic conditions. Different oxygen concentrations in the

Table 1. Comparison of substrate specificities of BCO and SCO using different assays. The k_{cat} and apparent K_m for the steroid were measured at 25 °C using 500 mM (tests 2 and 4) and 100 mM (tests 3 and 5) potassium phosphate buffer, pH 7.5, at air saturation. The corresponding values determined by polarography (oxygen-consumption) assay under similar experimental conditions (test 1) are reported in parentheses. The structures of the steroids used are shown in Fig. 1.

	Phosphate buffer (500 mM)				Phosphate buffer (100 mM)			
	Test 2[a]		Test 4[b]		Test 3[c]		Test 5[d]	
Substrate	k_{cat} (s^{-1})	K_m (mM)	k_{cat} (s^{-1})	K_m (mM)	k_{cat} (s^{-1})	K_m (mM)	k_{cat} (s^{-1})	K_m (mM)
BCO								
Cholesterol	106 (56)	0.2 (0.11)	26	1.6	48	0.07	48 (42)	0.04 (0.11)
trans-Dehydroandrosterone	0.6	0.6	0.2	2.6	0.8	1.2	1.0	0.9
Pregnenolone	44	0.9	12	2.1	21	0.4	35	0.2
Androstensulphate	0.05	1.4	0.02	3.4				
Cholestanol			12	0.6			40	0.02
trans-Androsterone			0.1	1.5			0.8	0.8
SCO								
Cholesterol	271 (10.6)	2.2 (0.26)	2	0.4	63	0.8	31	0.4
trans-Dehydroandrosterone	22	0.1	0.9	0.1	8.2	0.3	6.0	0.2
Pregnenolone	82	0.3	3	0.08	24	0.2	21	0.2
Androstensulphate	0.6	0.2	0.2	1.5				
Cholestanol			6	0.8			37	0.7
trans-Androsterone			0.7	0.2			7	0.5

[a] Product formation followed at 240 nm in the presence of 20 μL H_2O_2 (diluted 20-fold) and 0.625 $\mu g\cdot mL^{-1}$ catalase. [b] H_2O_2-production assayed using 4 $mg\cdot mL^{-1}$ of 3,5-dichlorosulphonate, 0.8 $mg\cdot mL^{-1}$ of 4-aminoantipyrine and 2 $\mu g\cdot mL^{-1}$ of HRP. [c] As test 2 but the substrate was dissolved in Triton X-100. [d] Test 5: H_2O_2-production assayed using 0.16 $mg\cdot mL^{-1}$ (in water) of *o*-dianisidine and 10 $\mu g\cdot mL^{-1}$ of HRP.

re-oxidation mixture were obtained by equilibrating the buffer solutions with air (21% O_2), with commercially available N_2/O_2 mixtures (90/10, 50/50 by vol.) or with pure O_2. Anaerobiosis was obtained by repeated cycles of evacuation and flushing with O_2-free argon. Prior to the experiments, oxygen was removed from the stopped-flow apparatus with N_2 at 25 °C, and syringes were incubated with a dithionite solution for 10 h and then rinsed with deoxygenated buffer.

EMTN data were analysed according to the method described by Gibson *et al*. [14]. 'Program A' (from D. Ballou, University of Michigan) was used for data analysis and for fitting of kinetic traces; data representation employed either the Grafit (Elsevier-Biosoft) or KaleidaGraph (Synergy Software) programs.

RESULTS

Correspondence of results from different assays and substrate specificity

In a previous paper, SCO reaction rates were monitored by H_2O_2 assay (test 5), O_2 consumption (test 1) or spectrophotometrically (product formation, test 2) with cholesterol as substrate [4]. However, the turnover rates obtained with the

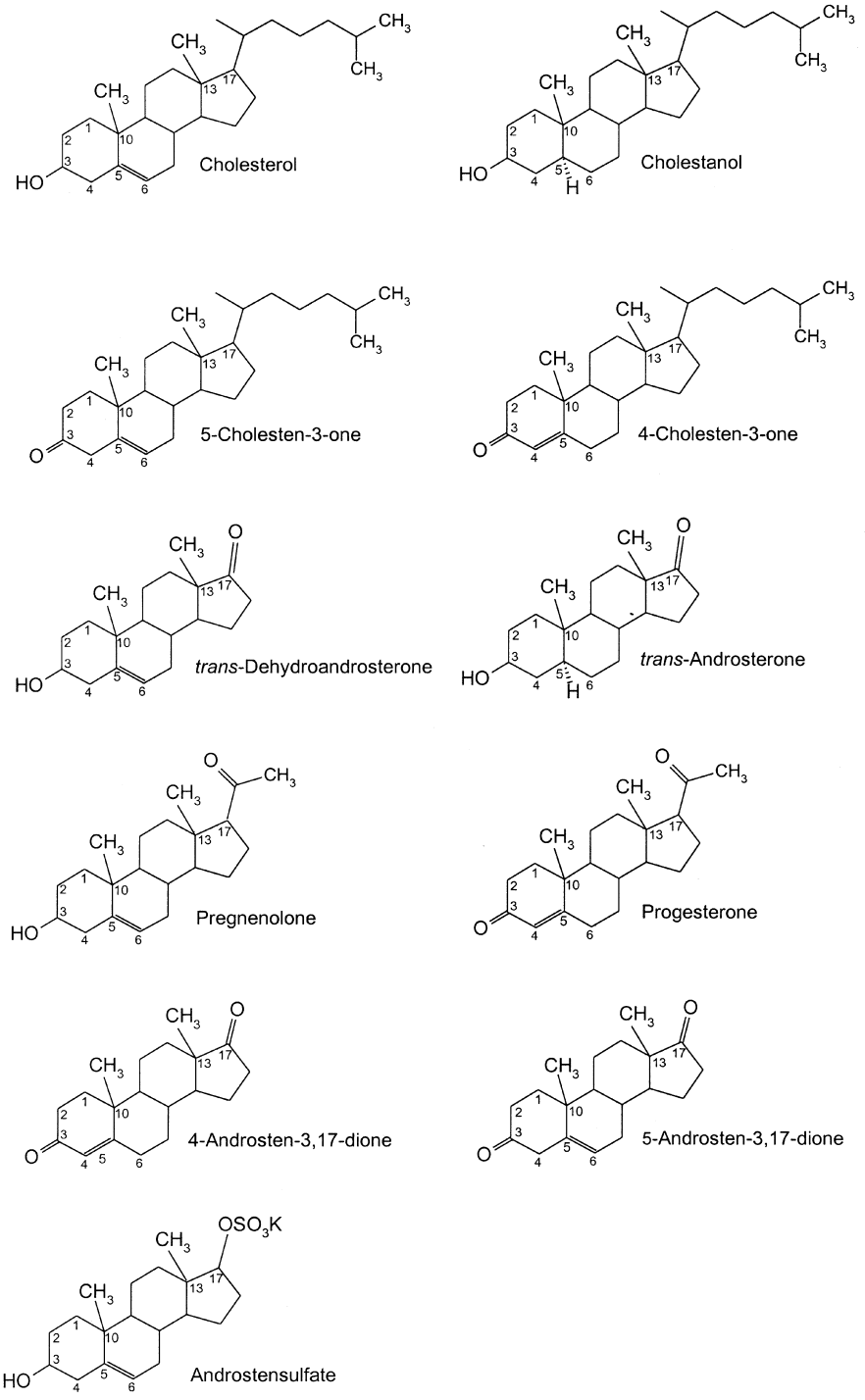

Fig. 1. Structures of steroids used in the present study.

Table 2. Substrate specificity of SCO with various alcohols as substrates. Measurements were performed at 25 °C in 100 mM potassium phosphate buffer, pH 7.5, following the decrease in 467 nm absorbance anaerobic conditions.

Substrate	Concentration (M)	$t_{1/2}$ (min^{-1})
Methanol	2.5	1500
Ethanol	1.7	38
1-Propanol	1.3	13
2-propanol	1.3	86
Cyclohexanol	0.00036	490
Benzyl alcohol	0.040	10

H_2O_2 assay were ≈50% lower than those determined by O_2 consumption. It was assumed that any one of several factors, including buffer concentration and the nature and concentration of the detergent(s), could be responsible for this, therefore the kinetic parameters of BCO and SCO were re-investigated using the steroid substrates and conditions listed in Table 1. From Table 1 it is evident that the discrepancy was not a function of substrate structure and that at 100 mM phosphate concentration the findings of the two sets of tests coincide. It was concluded that phosphate concentration substantially affects enzyme activity and subsequent experiments were carried out at a phosphate concentration of = 50–100 mM, a range in which the enzymatic activity of both COs did not vary. Full data on the effect of buffer concentration on CO activity will be reported elsewhere [5].

Effects of substrate structure on activity

Progesterone, 5-androsten-3,17-dione and 4-androsten-3,17-dione (see Fig. 1 for structures of substrates used in this work) are not substrates of BCO or SCO, as oxygen consumption was not observed by polarographic assay at 1.5 mM steroid concentration under various conditions. These substances did not inhibit BCO or SCO activity with cholesterol as the substrate. These results, and the data reported in Table 1, confirm that the two enzymes are specific for steroid substrates with an OH group in position C3 and that they show a marked

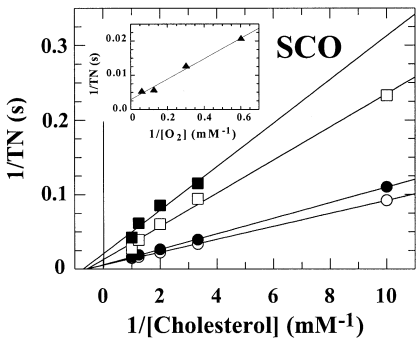

Fig. 2. Steady-state data for SCO with cholesterol as substrate and as a function of oxygen concentration. Measurements were made at 25 °C in 50 mM potassium phosphate buffer, pH 7.5, containing 1% Thesit and 10% 2-propanol. H_2O_2 formation was detected with *o*-dianisidine and HRP (test 5). (■) 0.120 mM, (□) 0.253 mM, (●) 0.602 mM and (○) 1.205 mM O_2 (all final concentrations). Main figure: Lineweaver–Burk representation. Inset: secondary plot of the ordinate intercepts of the main figure.

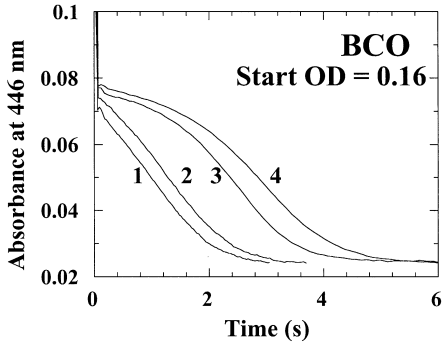

Fig. 3. Determination of turnover data for BCO with cholesterol using a stopped-flow instrument. The enzyme (6.3 μM) reacted with 1 mM (1), 0.8 mM (2), 0.5 mM (3) and 0.4 mM (4) cholesterol in 50 mM potassium phosphate buffer, pH 7.5, containing 1% Thesit and 10% 2-propanol, at 0.125 mM O_2 (all final concentrations). The traces represent the course of the reaction, monitored at 446 nm.

preference for steroids with at least a C_2 chain at position C17. Alcohols are effective detergents and are useful for solubilizing steroid substrates [4]. However, it was important to determine their behaviour as substrates with the enzymes being investigated. The alcohols listed in Table 2 are substrates for SCO. Incubation of oxidized SCO with 2-propanol under anaerobic conditions resulted in flavin reduction, as shown by the progressive disappearance of the 467 nm band of the oxidized chromophore, and by the formation of the typical absorption spectrum of the reduced enzyme. The course of this anaerobic

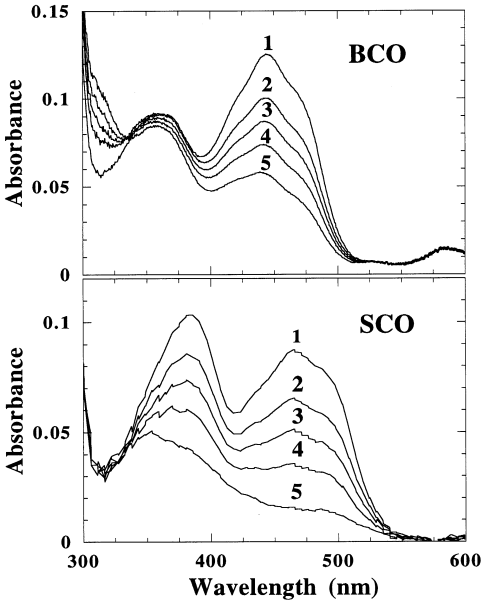

Fig. 4. Spectral courses of the anaerobic reduction of BCO and SCO by cholesterol followed in a stopped-flow spectrophotometer. BCO: 5 μM enzyme in 50 mM potassium phosphate buffer, pH 7.5, containing 1% Thesit and 10% 2-propanol was mixed anaerobically with 0.05 mM cholesterol (final concentrations). Spectrum (1) at 30 ms, is essentially unreacted enzyme (2) 60 ms, (3) 82 ms, (4) 185 ms and (5) 2.0 s after mixing. SCO: 4.5 μM enzyme in 50 mM potassium phosphate buffer, pH 7.5, containing 1% Thesit and 10% 2-propanol mixed anaerobically with 0.05 mM cholesterol (final concentrations). Spectrum (1) at 30 ms, is essentially unreacted enzyme (2) 100 ms, (3) 150 ms, (4) 225 ms and (5) 1.0 s after mixing.

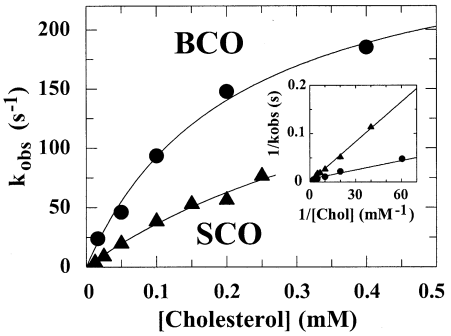

Fig. 5. Dependence of the observed rate of anaerobic reduction of BCO (●) and SCO (▲) on cholesterol concentration. Conditions: 50 mM potassium phosphate buffer, pH 7.5, 1% Thesit and 10% 2-propanol. Inset: double-reciprocal plots of the same data.

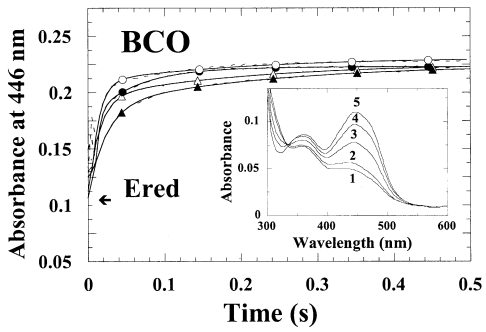

Fig. 6. Course of re-oxidation of free reduced BCO followed in a stopped-flow spectrophotometer. Main figure: time courses of reaction of 5.0 μM BCO (recorded at 446 nm) after mixing with buffer saturated with 5% (▲), 10.5% (△), 25% (●) and 50% (○) oxygen (final concentrations). The dashed lines represent the experimental traces, and the continuous lines are corresponding best fits obtained using a mono-exponential algorithm. Inset: the spectral course of re-oxidation after mixing with air-saturated (21% O_2) buffer. Spectra were recorded ≈1.5 ms (1), 10 ms (2), 25 ms (3), 100 ms (4) and 1.99 s (5) after mixing. Conditions: 50 mM potassium phosphate buffer, pH 7.5, containing 1% Thesit and 10% 2-propanol at 25 °C.

reaction was the same as that observed with cholesterol as the substrate (see below and Fig. 4) but was much slower. The reduction half-time depended markedly on the alcohol concentration and substituent(s), with a preference for compounds with an aromatic ring. Alcohols such as 2-propanol are convenient for generating reduced SCO via their simple addition to anaerobic enzyme solution; the flavin of BCO was not reduced under similar conditions.

The Δ5-6→Δ4-5 isomerization reaction

The conversion of 5-cholesten-3-one, the assumed intermediate, into 4-cholesten-3-one, the final product (see Fig. 1 for structures) was followed by monitoring the changes in absorbance at 240 nm which accompany it. Thus, with SCO at pH 7.5, in 50 mM phosphate buffer containing 1% Thesit and 1.25% 2-propanol, the turnover number (k_{cat}) was ≈ 670 s^{-1} (K_m ≈ 3.9 mM). The isomerization rate slowed to half at 500 mM [phosphate] (k_{cat} ≈ 330 s^{-1}, K_m ≈ 1.5 mM). Under the same conditions the activity of BCO was closely similar (k_{cat} ≈ 250 s^{-1}, K_m ≈ 0.3 mM). Importantly the rate of the isomerization catalysed by the reduced form of SCO (produced by addition of 2-propanol to anaerobic solution) was ≈2000 times slower. Comparison of the rates of 5-cholesten-3-one isomerization with those for the oxidation of cholesterol (Tables 1, 3 and 4; see below), showed that for neither enzyme was the Δ5-6→Δ4-5 isomerization rate-limiting, in agreement with Gadda *et al*. [4].

Steady-state measurements

The catalytic mechanism of both COs with cholesterol was studied using an H_2O_2 assay (test 5) and EMTN under the conditions shown in Tables 3 and 4.

SCO. The double-reciprocal plot in Fig. 2 shows a set of lines converging on the negative abscissa. Variation of the amount of detergent and alcohol in the assay mixture in some cases led to the line pattern tending to become parallel. This behaviour is compatible with formation of a ternary complex, with some of the rate constants sufficiently small that the bimolecular term Φ_{SO_2} of the steady-state equation becomes negligible at high substrate concentrations (Eqn 1):

$$\frac{e_t}{v} = \Phi_o + \frac{\Phi_S}{[Chol]} + \frac{\Phi_{O_2}}{[O_2]} + \frac{\Phi_{SO_2}}{[Chol][O_2]} \qquad (1)$$

where: $k_{cat} = 1/\Phi_o$; $K_m^{Chol} = \Phi_S/\Phi_0$; $K_m^{O_2} = \Phi_{O2}/\Phi_o$.

Table 3. Specific steady-state coefficients for the reaction of SCO with cholesterol as substrate determined using different assays. Measurements were 25 °C in 50 mM potassium phosphate buffer, pH 7.5. The steady-state values are taken from slopes and intercepts as reported in Fig. 1 according to the method of Dalziel [28]. Assay methods: (A) rate of H_2O_2 formation with *o*-dianisidine and HRP (test 5); (B) EMTN method. The calculated values obtained using the steady-state equation for the sequential mechanism (eqns 1 and 9–12) and the rate constants reported in Tables 5 and 6, are reported in parentheses.

Assay	Conditions	Lineweaver–Burk pattern	$\Phi_0^{-1} = k_{cat}$ (s^{-1})	Φ_S ($Ms \times 10^{-6}$)	Φ_{O_2}	Φ_{SO_2} ($M^2s \times 10^{-9}$)	K_m^{Chol} (mM)	$K_m^{O_2}$
A	no Thesit, no. 2-propanol[a]	≈parallel	28.0	7	19	n.d.	0.20	0.53
	1% Thesit, 1% 2-propanol	convergent	140	4	1.4	29.5	0.57	0.20
	1% Thesit, 10% 2-propanol	convergent	345	7	2.2	3.0	2.41	0.76
	10% Thesit, 5% 2-propanol	≈ parallel	15.8	94	38.5	n.d.	1.13	0.61
B	1% Thesit, 1% 2-propanol	convergent	67.6	0.5	25.2	3.0	0.04	1.75
	1% Thesit, 10% 2-propanol	≈ parallel	202.2	4.5	4.6	n.d.	0.91	0.92
			(231.8)	(2.4)	(3.9)	(≈0)	(0.56)	(0.90)
	10% Thesit, 10% 2-propanol	≈ convergent	3.2	11.2	46.8	5.0	0.04	0.15

[a] 100 mM potassium phosphate buffer.

Table 4. Specific steady-state coefficients for reaction of BCO with cholesterol determined by assays noted in Table 3. Measurements were in 50 mM potassium phosphate buffer, pH 7.5 at 25 °C. The calculated values obtained from the steady-state equation for the ping-pong mechanism, the data reported in Tables 5 and 6, and a k_5 value of ≈ 200 s^{-1} are reported in parentheses.

Assay	Conditions	Lineweaver–Burk pattern	$\Phi_0^{-1} = k_{cat}$ (s^{-1})	Φ_S (Ms × 10^{-6})	Φ_{O_2}	K_m^{Chol} (mM)	$K_m^{O_2}$
A	no Thesit, no 2-propanol	parallel	48.0	20.9	3.5	0.11	0.165
B	1% Thesit, 1% 2-propanol	≈ parallel	19.2	1.2	12.4	0.21	0.135
	1% Thesit, 10% 2-propanol	parallel	104.5	8.6	2.0	0.87	0.107
			(108)	(8.3)	(1.9)	(1.0)	(0.217)

The corresponding values of k_{cat}, K_m^{Chol} and $K_m^{O_2}$ as functions of Thesit and 2-propanol concentrations are given in Table 3; they show that these two compounds have strong effects on k_{cat} and K_m for cholesterol while the K_m for O_2 is affected less.

The steady-state kinetic behaviour of SCO was also investigated using EMTN. The oxidized enzyme was mixed aerobically with cholesterol and the change in flavin absorption was monitored at 467 nm. A very rapid decrease in absorption was observed, amounting to ≈60% of the total change. From this we deduced that the rate of enzyme reduction was ≈45% of its re-oxidation rate under the same conditions. Thus, the steady-state coefficients for cholesterol and O_2 determined by EMTN at 1% Thesit and 10% 2-propanol had practically the same numerical values (Table 3). The initial decrease of absorption was followed by a stationary phase, whose duration depended on the initial cholesterol concentration, and which leads to the fully reduced enzyme as the final state. An approximation to a steady-state phase was observed only in a narrow range of substrate The 467 nm traces were analysed as a function of oxygen concentration according to Gibson *et al.* [14], and the kinetic parameters obtained are given in Table 3. There was good agreement between these values and those obtained for the H_2O_2 assay (test 5). The approximately two-fold difference between the two assays for k_{cat} values might be due to differences in final enzyme concentration, which ranged from 0.01 to 0.1 μM for the H_2O_2 method to 10–20 μM for EMTN. A similar effect of enzyme concentration on k_{cat} has been reported previously, e.g. for D-amino acid oxidase [17].

The k_{cat} values also depended on the concentrations of Thesit and 2-propanol (both required to solubilize cholesterol). Briefly, increase in Thesit up to 0.2% resulted in increased SCO activity, followed by a sharp decrease. Increase in 2-propanol had a similar effect on SCO activity, which was evident mainly as a change in K_m^{Chol} The ionic strength of the buffer also had an effect (see Table 1, and [5]).

BCO. The reaction of BCO with cholesterol was studied using EMTN (Fig. 3) and by monitoring H_2O_2 production (test 5). The results differed from those obtained for SCO in that Lineweaver–Burk plots always gave parallel lines (Table 4) suggesting that a ping-pong mechanism is active. An increase in [2-propanol] from 1.25% to 10% did not alter k_{cat} (51 s^{-1} vs. 50.8 s^{-1}) at a fixed oxygen concentration (0.253 mM) in the presence of 1% Thesit and 500 mM potassium phosphate buffer. Phosphate concentration had a limited effect: an increase from 50 to 500 mM resulted in a three-fold increase in k_{cat} (data not shown). The effect of [2-propanol] on K_m^{Chol} was much smaller for BCO than SCO and was more evident on the Φ_{O2} steady-state coefficient (Table 4).

The reductive half-reaction

When oxidized forms of BCO and SCO were mixed anaerobically with cholesterol at 25 °C and pH 7.5, the yellow colour bleached rapidly to yield the typical spectrum of the reduced enzyme (Fig. 4; [4]). The time course was followed at 446 nm for BCO and 467 nm for SCO, and in both cases was represented satisfactorily by a single exponential curve. In all conditions, the observed reduction rates, k_{obs}, exhibited saturation with increasing cholesterol concentration (Fig. 5). This was interpreted as follows:

$$\text{E-FAD}_{ox} + \text{Chol} \underset{k_{-1}}{\overset{k_1}{\Leftrightarrow}} \text{E-FAD}_{ox}$$

$$\sim \text{Chol} \underset{k_2}{\overset{k_1}{\Leftrightarrow}} \text{E-FAD}_{red} \sim \text{5-chol-3one} \qquad (2)$$

Table 5. Specific rate constants obtained for reductive half-reaction of BCO and SCO with cholesterol as substrate in stopped-flow experiments. Measurements were in 50 mM potassium phosphate buffer, pH 7.5, at 25 °C with different Thesit and 2-propanol concentrations.

Conditions		k_{red} (k_2) (s^{-1})	K_d (≈k_{-1}/k_1) (mM)	Calculated[a] k_1 ($M^{-1}s^{-1}$)	Calculated[a] k_{-1} (s^{-1})	1/slope (≈$k_2 \cdot k_{-1}/k_1$) (M^{-1} s^{-1})(×10^6)
SCO	1% Thesit, 1% 2-propanol	5.5	0.12	350 000	60	22.0
	1% Thesit, 10% 2-propanol	231.8	1.5	500 000	2500	5.5
	5% Thesit, 5% 2-propanol	55.3	1.88	500 000	2500	35.8
	10% Thesit, 5% 2-propanol	46.1	1.67	500 000	2500	34.8
BCO	1% Thesit, 1% 2-propanol	5.7	0.082	240 000	60	15.2
	1% Thesit, 10% 2-propanol	235.1	0.158	770 000	1250	16.7

[a] The k_1 and k_{-1} rate constants are the minimal values determined by computer simulation of the experimental traces using program A and eqn 2 (Dave Ballou, University of Michigan).

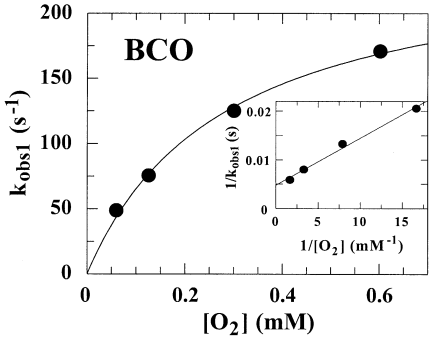

Fig. 7. Dependence of the observed rate of re-oxidation of reduced BCO on oxygen concentration. The reduced form of BCO (7.0 μM) was obtained by anaerobic incubation with 1.5-fold excess cholesterol. This solution was then mixed with buffer solutions equilibrated with 10, 21, 50 and 100% O_2, The data points are the average of five single measurements of the first phase (k_{obs1}) determined using the stopped-flow instrument following the absorbance increase at 446 nm. Conditions: 50 mM potassium phosphate, pH 7.5, containing 1% Thesit and 10% 2-propanol, and at 25 °C.

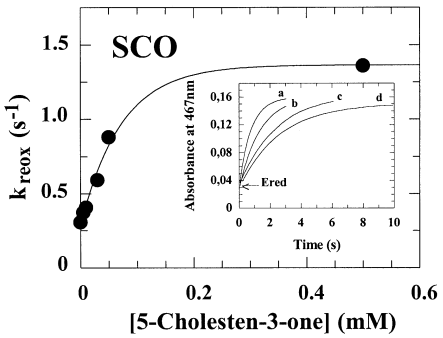

Fig. 9. Dependence of the observed rate of re-oxidation of reduced SCO with oxygen on concentration of 5-cholesten-3-one. Rates were determined using the stopped-flow method at 25 °C. The reduced form of SCO (7.9 μM) in anaerobic 50 mM potassium phosphate, pH 7.5, containing 1% Thesit and 10% 2-propanol was mixed with buffer solution containing various concentrations of 5-cholesten-3-one equilibrated with air, and the increase in absorbance at 467 nm was followed. Data points are averages of five determinations. Inset: traces of reaction course in presence of (a) 0.5, (b) 0.05, (c) 0.01 and (d) 0.0 mM 5-cholesten-3-one (all final concentrations).

Steps k_1 and k_{-1} were not observed spectrophotometrically, implying that substrate binding did not affect the oxidized flavin chromophore to a measurable extent. The disappearance of absorption therefore reflects step k_2. According to Strickland *et al*. [18], the linearity of the double-reciprocal plots of k_{obs} vs. [*S*] (inset of Fig. 5) is compatible with a situation in which $k_{-2} \ll k_2$ and $k_{-2} \approx 0$, i.e. a practically irreversible reduction step preceded by attainment of rapid equilibrium between free enzyme substrate bound enzyme, i.e: $k_{-1} > k_2$ (eqn 2).

Simulation of the experimental traces with program A (D. Ballou, University of Michigan) yielded a reasonable duplication of the absorbance changes using minimal values for k_1 of 770 000 $M^{-1}\cdot s^{-1}$ and 500 000 $M^{-1}\cdot s^{-1}$ for BCO and SCO, respectively (1% Thesit and 10% 2-propanol, see Table 5). The minimal value for k_{-1}, was 1250–2500 s^{-1} for both enzymes. Under the same experimental conditions, the extrapolated rates of reduction of BCO and SCO with cholesterol were similar: 235 and 232 s^{-1}, respectively (Table 5). With both COs, the rate of reduction was markedly dependent on the concentration of the alcohol employed to solubilize cholesterol. Thus an increase in 2-propanol concentration was paralleled by an increase in both k_{red} and K_d (Table 5). By contrast, Thesit did not influence SCO activity: the k_{red} and K_d values found at 5% and 10% Thesit concentrations were similar (Table 5, in the presence of 5% 2-propanol).

A feature of many flavin-dependent oxidases is that they form relatively stable reduced enzyme/product complexes, which often have characteristic charge transfer absorptions and can be detected spectrophotometrically [19]. For this reason, formation of the fully reduced uncomplexed species is often seen to follow a biphasic course. Typical cases are L-lactate oxidase and D-amino-acid oxidase [20,21]. By contrast, the reduction course of the COs subject of this study was essentially monophasic. This means that the reduced enzyme–5-cholesten-3-one complex or its dissociation are not detectable spectroscopically. We attempted to detect spectral changes during aerobic titrations of SCO with 4-cholesten-3-one by differential spectroscopy. In the presence of 25 mM product (plus 20% 2-propanol and 25% Thesit, to ensure solubility) there were only very minor absorption changes, evident as a decrease at 515 nm and an increase around 450 nm

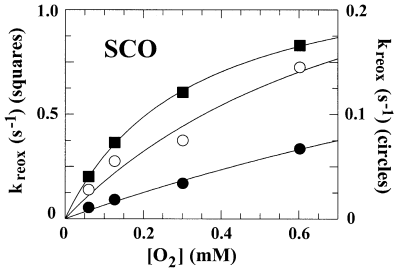

Fig. 8. Dependence of the observed rate of re-oxidation of reduced SCO on oxygen concentration, and effect of 2-propanol concentration. Free reduced SCO (7.1 μM) was reacted in a stopped-flow apparatus with solutions of 50 mM potassium phosphate buffer, pH 7.5, containing 1% Thesit, equilibrated with 10, 21, 50 and 100% O_2 at 25 °C. (●) No 2-propanol, (○) 1% 2-propanol and (■) 10% 2-propanol (all final concentrations).

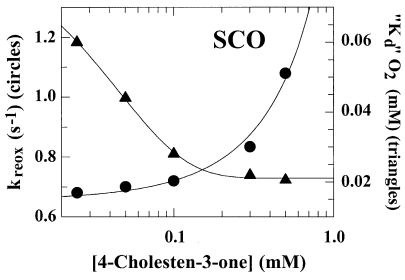

Fig. 10. Dependence of re-oxidation rate (●) and apparent K_d for oxygen (▲) of reduced SCO on 4-cholesten-3-one concentration. Reduced SCO (7.9 μM) was reacted in a stopped-flow apparatus with various concentrations of oxygen at 25 °C and pH 7.5 (as in Fig. 9). The k_{reox} values are the rates estimated at saturating oxygen concentration in the presence of the 4-cholesten-3-one concentrations shown.

Table 6. Specific rate constants obtained from stopped-flow experiments for re-oxidation of BCO and SCO. Measurements were in 50 mM potassium phosphate buffer, pH 7.5, at 25 °C with various Thesit and 2-propanol concentrations.

Conditions			Calculated					
			k_{conv} (s^{-1})	k_4 (= $1/\Phi_{O_2}$) ($M^{-1}\cdot s^{-1}$) ($\times 10^6$)	k_{-conv} (s^{-1})	k_{reox} (s^{-1})	$K_{d,app}$ (mM)	Slope (Ms) ($\times 10^{-6}$)
From reduced enzyme form:								
BCO[a]	1% Thesit, 1% 2-propanol	biphasic	245	0.08	32.5	0.39 (= k_4/k_{-conv})		0.59
	1% Thesit, 10% 2-propanol	biphasic	248	0.50	140	0.28 (= k_4/k_{-conv})		0.96
SCO	no Thesit, no. 2-propanol	monophasic (linear fitting)				0.24	1.60	5090 (103.4 M^{-1} s^{-1})
	1% Thesit, 1% 2-propanol	monophasic				0.27	0.62	1860
	1% Thesit, 10% 2-propanol	mono/biphasic				1.26	0.21	173
	10% Thesit, 5% 2-propanol	monophasic				0.77	0.01	11.4
From the complex with the product:								
SCO[b]	0.5 mM 5-cholesten-3-one	monophasic				1.40	0.006	3.9 ($\approx k_6$)
	0.025 mM 4-cholesten-3-one	monophasic				0.68	0.060	85.1
	0.05 mM 4-cholesten-3-one	monophasic				0.70	0.044	57.4
	0.1 mM 4-cholesten-3-one	monophasic				0.72	0.028	36.6
	0.3 mM 4-cholesten-3-one	monophasic				0.83	0.021	21.6
	0.5 mM 4-cholesten-3-one	monophasic				1.08	0.025	20.5

[a] According to the conversion mechanism between two different conformations of the reduced enzyme (eqns 3 and 4). [b] 50 mM potassium phosphate, pH 7.5, 1% Thesit and 10% 2-propanol.

(data not shown). Furthermore, the spectral changes induced by binding of 5-cholesten-3-one to oxidized SCO were also minor and consisted of a small increase in the visible portion of the absorbance spectrum ($\Delta\varepsilon_{max} < 1000\ M^{-1}\cdot cm^{-1}$). The results of anaerobic titration of fully reduced SCO (obtained by anaerobic reaction with excess 2-propanol) were similar in that only minor spectral changes were observed. In neither case was the effect modified by increasing Thesit or 2-propanol concentrations (final concentrations 10% Thesit and 10–20% 2-propanol). The small changes in absorbance and the limited solubility of the ligands prevented estimation of K_d values for formation of the enzyme–product complex.

The oxidative half-reaction

Free reduced BCO. The uncomplexed reduced form of BCO was reacted in the stopped-flow instrument with buffer containing 1% Thesit and various oxygen concentrations. Spectra were recorded during re-oxidation (Fig. 6). The absorption increase at 446 nm was biphasic in the presence of 1% and 10% 2-propanol. The observed rate for the second phase (k_{obs2}) of the reaction was insensitive to oxygen concentration ($k_{obs2} < 5\ s^{-1}$) and quite slow. By contrast, the rapid initial phase (k_{obs1}) showed saturation with increasing oxygen concentration (Fig. 7). It is not easy to interpret this finding, as the detection of an encounter complex of a reduced flavin enzyme with dioxygen preceding a chemical event would be unprecedented. The behaviour can be represented by eqn 3, in which one of the reactants is reversibly converted into the reactive species via k_{conv}:

$$\text{E-FAD}_{red}* \underset{k_{-conv}}{\overset{k_{conv}}{\Leftrightarrow}} \text{E-FAD}_{red} + O_2 \underset{k_{-4}}{\overset{k_4}{\Leftrightarrow}} \text{E-FAD}_{ox} \sim H_2O_2 \qquad (3)$$

The nature of k_{conv} could not be determined in the present study. Note, however, that the reaction system is complex: substrate, detergent and enzyme can form micelles, whose behaviour, particularly kinetic behaviour, is not known. The experiments illustrated in Fig. 10 (for SCO, see below) suggest that the accessibility or availability of reactive oxygen is influenced by micelle composition. Our finding of a biphasic reaction with oxygen, the initial phase of which is saturable, is compatible with interconversion between two forms of reduced BCO, only one of which (the second species, eqn 3) reacts efficiently with oxygen. Different environments within the micelle system could give these different enzyme forms. However, dioxygen-triggered interconversion between the unreactive and reactive forms, cannot be excluded from the present data, although this seems improbable. An estimation of the second order rate constant k_{obs1} of the oxygen reaction with reduced BCO was obtained from eqn 4, as described by Schopfer *et al.* [22].

$$k_{obs1} = \frac{k_{conv}\cdot k_4\cdot[O_2] + k_{-4}\cdot(k_{conv} + k_{-conv})}{k_{-conv} + k_4\cdot[O_2] + k_{-4}} \qquad (4)$$

If $k_{-4} \approx 0$ (as for the reaction of most reduced flavoproteins with O_2), it follows that:

$$k_{obs1} = (k_{conv}\cdot k_4\cdot[O_2])/(k_{-conv}\cdot k_4\cdot[O_2]) \qquad (5)$$

This equation describes hyperbolic (saturating) dependence of k_{obs1} on oxygen concentration, as shown in Fig. 7, where the *y*-intercept of the corresponding double-reciprocal plot (Fig. 7, inset) corresponds to k_{conv}; the *x*-intercept (reciprocal of apparent K_d) corresponds to k_{conv}/k_4 and the slope is $k_{-conv}/(k_{conv}\cdot k_4)$ (Table 6). Based on the deduction (see above) of a ping-pong mechanism for the reaction of BCO with cholesterol and oxygen, the steady-state coefficient Φ_{O_2} corresponds to $1/k_4$ (eqn 8). This allows estimation of the values of k_{conv} and k_{-conv} (Table 6).

Free reduced SCO. The experimental traces for reaction of reduced uncomplexed SCO with O_2 under conditions similar to those used for BCO closely fitted a single exponential rate process, i.e. they were essentially monophasic. In the absence of 2-propanol and Thesit, re-oxidation rates depended linearly on oxygen concentration and extrapolated to the origin, consistent with a second order reaction in dioxygen. By contrast, in the presence of 1% Thesit and 1% or 10% 2-propanol, the plots showed saturation behaviour to oxygen (Fig. 8 and Table 6). Both 2-propanol and Thesit increased the apparent rate of re-oxidation and decreased the apparent K_d for oxygen, although Thesit had a larger effect on the K_d (Table 6). For all cases, and in particular for the linear dependence obtained in the absence of 2-propanol, the observed rates of re-oxidation were too slow to be significant in turnover (Table 3). For this reason, accurate evaluation of the second-order rate constants for the reaction of reduced enzyme with oxygen in the presence of surfactants was not possible.

Reduced SCO–product complex. As observed above, rate of re-oxidation of free reduced SCO was too slow to be important in catalysis, it is therefore likely that the important step in re-oxidation involves reduced enzyme bound either to the intermediate 5-cholesten-3-one, or the final product 4-cholesten-3-one. Unfortunately, a reduced enzyme–5-cholesten-3-one complex cannot be produced experimentally, as it rearranges to 4-cholesten-3-one in the presence of the enzyme [4]. We therefore performed kinetic observations on the reaction of reduced uncomplexed enzyme, obtained by overnight incubation with 2-propanol, with buffer containing both 5-cholesten-3-one and oxygen. We assumed that the ligand would bind faster than any ensuing oxygen reaction. Under these conditions the absorbance increase at 467 nm was essentially monophasic (Fig. 9, inset), and the plots of the primary data revealed apparent saturation at increasing dioxygen concentration. The re-oxidation rate at 0.125 mM O_2 reached apparent saturation at ≈ 0.5 mM 5-cholesterol-3-one (Fig. 9); although this rate of re-oxidation was 5.8 times higher than in the absence of ligand, it was too slow to be significant in turnover. Presence of the ligand had a stronger effect on the apparent K_d for O_2 lowering it by 40 times compared with that for the free reduced enzyme (Table 6).

Re-oxidation of reduced SCO was investigated with the final product, 4-cholesterol-3-one, present in the concentration range 0.025–0.5 mM. We observed an increase in k_{reox} and a corresponding decrease in the apparent K_d for oxygen with increasing product concentration (Fig. 10). This behaviour is diagnostic for the formation of a dioxygen reactive E_{red}–product complex but, as was the case for the binding experiments with SCO, saturation could not be achieved due to the low solubility of 4-cholesten-3-one (0.5 mM is close to the limit of solubility). The critical micelle concentrations of 5-cholesten-3-one and 4-cholesten-3-one (110 μM and 135 μM, respectively) in the presence of 50 mM potassium phosphate buffer, pH 7.5, containing 1% Thesit and 10% 2-propanol, were ≈10 times higher than for cholesterol (15 μM) under the same conditions. Interestingly, both k_{reox} plots as function of concentration of intermediate and product (Figs 9 and 10) showed a curvature at concentrations corresponding to the critical micelle concentration for the steroid, suggesting a strong effect of micelle formation on the re-oxidation process.

DISCUSSION

Substrate specificity

Our findings on substrate specificity for the two enzymes are consistent with those on COs from *Nocardia, Streptomyces violascens* and *Streptoverticillum cholesterolicum* [23–25]. Specifically an -OH at position 3 is necessary for steroids to be substrates. However, a double bond on the steroid B-ring is not mandatory because both SCO and BCO used cholestanol and *trans*-androsterone as substrates (Table 1 and Fig. 1). The structures of these compounds are similar to cholesterol and *trans*-dehydroandrosterone but lack 5–6 unsaturation. For optimal activity a C(17)-tail, including at least one C2 unit also appears to be necessary. Recently a mutant of *Brevibacterium* CO (containing noncovalent FAD) was obtained by deleting residues 79–83, which form a surface loop [12] and appear to cap the active site [1,2]. The kinetic properties of this mutant suggested that the loop is important in packing the cholesterol tail and in determining specificity towards C(17) substituents. This loop is also considered important for extracting cholesterol from the membrane, but is not the primary determinant of affinity for vesicles [12]. By comparison of the parameters of cholesterol oxidation with those for isomerization of 5-cholesten-3-one (Tables 3 and 4) it is apparent that isomerization is not rate-limiting for either enzyme. However, it is the oxidized forms of the enzymes that are competent in isomerization catalysis.

From the three-dimensional structure of a related BCO with noncovalently bound FAD [1,2] it can be inferred that the functional group involved is probably Glu361 (numbering of noncovalent BCO). Because isomerization involves abstraction of the C(4)-H as H^+ by anionic carboxylate [26], the difference in isomerisation rate between the oxidized and reduced forms of the enzyme probably reflects this group being ionized in the oxidized form and neutral in the reduced form. This is in agreement with studies by Kass and Sampson [26] in which product composition was analysed using deuterated and nondeuterated substrates.

The reductive half-reaction

The converging lines for SCO in Lineweaver–Burk plots in the presence of 1% Thesit and 10% 2-propanol (Fig. 2) are diagnostic of a ternary complex mechanism. Some of the rate constants were small enough to produce a parallel pattern under some experimental conditions (Table 3). By contrast double reciprocal plots were always parallel for BCO. Because the reductive half-reaction is practically irreversible ($k_2 \gg k_{-2}$) parallel plots are to be expected (eqn 2 and right-hand side of Fig. 11). The validity of a binary complex mechanism for BCO is supported by the results of primary trace simulations, where superimposition of the experimental and calculated traces requires that $k_{-2} \approx 0$ (not shown). Similar simulations allowed estimation of the lowest limits for k_1 and k_{-1} listed in Table 5. For both enzymes, and under all experimental conditions, the enzyme–substrate complex was essentially in equilibrium with the enzyme plus substrate, i.e. $k_{-1} \gg k_2$ (Fig. 11). Based on this situation, the ordinate intercept of the double-reciprocal plot of the reduction rates for both COs, e.g. the one reported in the inset of Fig. 5, yields $1/k_2$ and the slope $k_{-1}/k_1 \cdot k_2$. In this case, the ratio of slope to intercept yields K_d (k_{-1}/k_1) [18]. The finding of a rapid pre-equilibrium condition also enables us to interpret product binding in the re-oxidation experiments as discussed below.

It is important to note that the rates of reduction in the presence of 1% Thesit and 1% 2-propanol (Table 5) were significantly lower than the k_{cat} values for the enzymes under the same experimental conditions (Tables 3 and 4). Furthermore, the cholesterol concentrations used in reductive half-reaction and EMTN experiments, under different experimental conditions, were always higher than the critical micelle concentrations for cholesterol (40 μM at 1% Thesit and 1% 2-propanol, and 15 μM at 1% Thesit and 10% 2-propanol).

The oxidative half-reaction

A major finding of this study is that the apparent rates of re-oxidation of reduced SCO were not consistent with the turnover rates. In general, the double-reciprocal plots of the observed rates of re-oxidation of BCO and SCO as function of oxygen concentration yielded straight lines with a definite intercept on the ordinate in the absence and presence of both intermediate and final product as ligands. In general such behaviour is taken to indicate the presence of definite intermediates (presumably covalent oxygen adducts) preceding re-formation of oxidized flavin. However, absorption spectra recorded during re-oxidation provide no indication of such

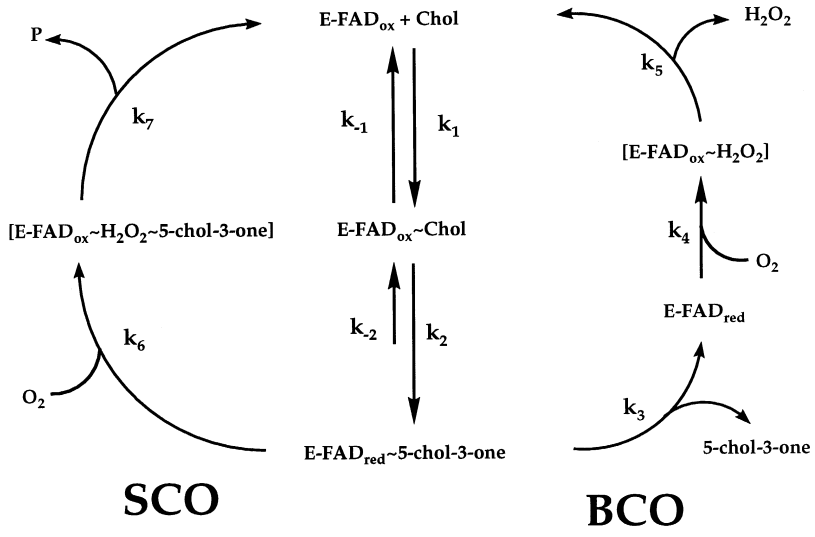

Fig. 11. Kinetic mechanisms for SCO and BCO. Intermediates not detected spectrally, but required by the kinetic mechanism, are shown in parentheses.

intermediates (see Fig. 6 for BCO). The interpretation of these data thus yields a dilemma. In general terms, such a behaviour could be due to any kind of rate-limiting process preceding the formation of oxidized flavin. Assuming the absence of flavin–oxygen intermediates, such a step would have to precede the reaction with dioxygen. Changes such as conformational ones involving the complex between the reduced enzyme intermediate/product prior to reaction with dioxygen can explain the kinetic mechanism (see Eqn (3) for BCO). A further possibility would be for the rate of oxygen or enzyme 'escape' from micelles, i.e. its availability, to be limiting. Against this variant argues the finding that under the same experimental conditions the two enzymes show completely different rates of re-oxidation at a saturating oxygen concentration (Table 6) and that the oxygen solubility in water and in a solution containing 1% Thesit and 10% 2-propanol is practically identical. This variant would hold, however, if the enzyme itself would be constituent part of a micelle system, and if the two enzymes would differ in this context. The discrepancy between the rate of re-oxidation and the turnover rates determined under the same experimental conditions could arise from the presence of micelles in the solutions used for the reductive half-reaction and EMTN measurements due to the presence of cholesterol.

The overall mechanism

Based on the experimental data we propose a ping-pong mechanism (binary complex mechanism) for the oxidation of cholesterol by BCO. With such a model the general steady-state kinetics equation (eqn 1) can be simplified for the absence of the bimolecular term (Φ_{SO_2}). The remaining terms would be:

$$\Phi_0 = (1/k_2 + 1/k_5 + 1/k_3)$$

$$\approx (k_2 + k_5)/k_2{\cdot}k_5 \text{ (if } k_3 >> k_2 \text{ and } k_5) \quad (6)$$

$$\Phi_S = (k_{-1} + k_2)/k_1{\cdot}k_2 \quad (7)$$

$$\Phi_{O_2} = 1/k_4 \quad (8)$$

To test validity of this model we compared the values obtained using the model, assuming the value of $\approx 200\ s^{-1}$ for k_5 (constant for H_2O_2 dissociation from re-oxidized enzyme), with the values observed for BCO in steady-state turnover in the presence of 1% Thesit and 10% 2-propanol (Table 5). The numerical value of the Φ_0 term is $\approx$50% of that of k_{red} determined under the same experimental conditions. This is a situation where both terms (k_2 and k_5) contributing to Φ_0 have similar numerical values.

As noted previously, the data for SCO clearly indicate a ternary complex mechanism, with the Φ_{O_2} term having a numerical value similar to that of the slope of the double-reciprocal plot of the re-oxidation reaction in the presence of 0.5 mM 5-cholesten-3-one. In fact, the rate of re-oxidation estimated for the reduced SCO in its free form, as well as in the presence of various concentrations of 5-cholesten-3-one and 4-cholesten-3-one (Table 6), was significantly slower than the turnover rate determined under steady-state conditions (Tables 3 and 5). In the presence of 1% Thesit and 10% 2-propanol, the reductive half-reaction is largely rate-limiting, as suggested by the similar values of k_{cat} and k_2 (the rate of reduction). This indicates that the rate of product dissociation from the ternary complex with enzyme in the oxidized form (k_7 of Fig. 11) is very fast and does not affect the turnover number ($\Phi_0 \approx 1/k_2$). This is an important difference compared with BCO, where the release of H_2O_2 influences the turnover number [$\Phi_0 = (k_2 + k_5)/k_2{\cdot}k_5$]. Taken together, the results of the rapid kinetic studies with SCO are consistent with an ordered sequential mechanism:

$$\Phi_0 = (k_7 + k_2)/k_2{\cdot}k_7 \approx 1/k_2 \text{ (if } k_7 >> k_2) \quad (9)$$

$$\Phi_S = (k_{-1} + k_2)/k_1{\cdot}k_2 \quad (10)$$

$$\Phi_{O_2} = 1/k_6 \quad (11)$$

$$\Phi_{SO_2} = (k_{-1} + k_{-2})/k_1{\cdot}k_2{\cdot}k_6 \approx \text{zero.} \quad (12)$$

The problems in interpreting the results of the oxidative half-reaction for both COs may be resolved by considering the influence of micelles on the kinetics of the enzymes [27] and in particular the differential partitioning of substrates and other species involved in the catalysis between micelles and the bulk phase. In the reductive half-reaction experiments, conditions were closer to those encountered *in vivo* due to the presence of cholesterol micelles. By contrast in the 're-oxidation' experiments, cholesterol was absent and there were no cholesterol micelles. This could explain the low re-oxidation rates found for the free reduced enzyme and the difficulty in obtaining complete formation of the E_{red}–P complex during titration experiments. The kinetic of chemical reactions catalysed by enzymes in the presence of micelles of amphiphilic compounds in organic solvents obey the classical Michaelis–Menten equation although a partition of substrate between the pseudophases of micelles and the bulk phase of organic solvent should be taken into account. The problems in obtaining reasonable values for the oxidative half-reaction of SCO in the presence of products can be ascribed to the differences in micellar organization between the solution containing the products (due to their high value of critical micelle concentration) and the solution containing cholesterol. The lack of agreement observed between the reductive half-reaction rate constants and the EMTN steady-state coefficients in the presence of 1% Thesit and 1% 2-propanol can be similarly explained. In the latter case the experimental conditions (50 mM potassium phosphate buffer, pH 7.5, 1% Thesit and 10% 2-propanol), were such that the critical micelle concentration for cholesterol was low.

Finally, we have shown that the oxidized forms of both COs are those which perform the isomerization. With SCO a ternary complex consisting of re-oxidized enzyme and products is formed, consistent with the proposed sequential mechanism.

ACKNOWLEDGEMENTS

We thank Roche Diagnostics for the generous supply of CO. This work was supported by grants from Italian MURST to L.P. and M.P.

REFERENCES

1. Li, J., Vrielink, A., Brick, P. & Blow, D.M. (1993) Crystal structure of cholesterol oxidase complexed with a steroid substrate: implications for flavin adenine dinucleotide dependent alcohol oxidases. *Biochemistry* **32**, 11507–11515.
2. Vrielink, A., Lloyd, L.F. & Blow, D.M. (1991) Crystal structure of cholesterol oxidase of *Brevibacterium sterolicum* refined at 1.8 Å resolution. *J. Mol. Biol.* **219**, 533–554.
3. Decker, K. (1991) Covalent flavoproteins. In *Chemistry and Biochemistry of Flavoenzymes*, Vol. II (Müller, F., ed.), pp. 343–393. CRC Press, Boca Raton, FL.
4. Gadda, G., Wels, G., Pollegioni, L., Zucchelli, S., Ambrosius, D., Pilone, M.S. & Ghisla, S. (1997) Characterization of cholesterol

oxidase from *Streptomyces hygroscopicus* and *Brevibacterium sterolicum*. *Eur. J. Biochem.* **250**, 369–376.

5. Pollegioni, L., Gadda, G., Ambrosius, D., Ghisla, S. & Pilone, M.S. (1999) Cholesterol oxidase from *Streptomyces hygroscopicus* and *Brevibacterium sterolicum*: effect of surfactants and organic solvents on activity. *Biotechnol. Appl. Biochem.* **30**, in press.
6. Allain, C.C., Poon, L.S., Chan, C.S.G., Richmond, W. & Fu, P.C. (1974) Enzymatic determination of total serum cholesterol. *Clin. Chem.* **20**, 470–475.
7. Purcell, J.P., Greenplate, J.T., Jennings, M.G., Ryerse, J.S., Pershing, J.C., Sims, S.R., Prinsen, M.J., Corbin, D.R., Tran, M., Douglas Sammons, R. & Stonard, R.J. (1993) Cholesterol oxidase: a potent insecticidal protein active against boll weevil larvae. *Biochim. Biophys. Res. Commun.* **196**, 1406–1413.
8. Smith, A.G. & Brooks, C.J.W. (1977) The substrate specificity and stereochemistry, reversibility and inhibition of the 3-oxo-steroid $\Delta 4-\Delta 5$-isomerase component of cholesterol oxidase. *Biochem. J.* **167**, 121–129.
9. Cheillan, F., Lafont, H., Termine, E., Fernandez, F., Sauve, P. & Lesgards, G. (1989) Molecular characteristics of the cholesterol oxidase and factors influencing its activity. *Biochim. Biophys. Acta* **999**, 233–238.
10. Medina, M., Vrielink, A. & Cammack, R. (1994) ESR and electron nuclear double resonance characterization of the cholesterol oxidase from *Brevibacterium sterolicum* in its semiquinone state. *Eur. J. Biochem.* **222**, 941–947.
11. Khmelnitsky, Y.L., Hilhorst, R. & Veeger, C. (1988) Detergentless microemulsion as media for enzymatic reactions. *Eur. J. Biochem.* **176**, 265–271.
12. Sampson, N.S., Kass, I.J. & Ghoshroy, K.B. (1998) Assessment of the role of Ω loop of cholesterol oxidase: a truncated loop mutant has altered substrate specificity. *Biochemistry* **37**, 5770–5778.
13. Croteau, N. & Vrielink, A. (1996) Crystallization and preliminary X-ray analysis of cholesterol oxidase from *Brevibacterium sterolicum* containing covalently bound FAD. *J. Struct. Biol.* **116**, 317–319.
14. Gibson, Q.H., Swoboda, B.E.P. & Massey, V. (1964) Kinetics and mechanism of action of glucose oxidase. *J. Biol. Chem.* **259**, 3927–3934.
15. Hsu, K.L. & Powell, G.L. (1975) Inhibition of citrate synthetase by oleolyl-CoA: a regulatory phenomenon. *Proc. Natl Acad. Sci. USA* **72**, 4729–4733.
16. Langkau, B. (1992) Studies with flavin coenzymes – catalytic mechanism of 2-amino benzoyl-CoA monooxygenase-reductase and of yeast D-amino acid oxidase. PhD Thesis, University of Konstanz.
17. Pollegioni, L., Langkau, B., Tischer, W., Ghisla, S. & Pilone, M.S. (1993) Kinetic mechanism of D-amino acid oxidase from *Rhodotorula gracilis* and *Trigonopsis variabilis*. *J. Biol. Chem.* **268**, 13850–13857.
18. Strickland, S., Palmer, G. & Massey, V. (1975) Determination of dissociation constants and specific rate constants of enzyme–substrate (or protein–ligand) interactions from rapid reaction kinetic data. *J. Biol. Chem.* **250**, 4048–4052.
19. Ghisla, S. & Massey, V. (1991) L-Lactate oxidase. In *Chemistry and Biochemistry of Flavoenzymes*, Vol. II (Müller, F., ed.), pp. 243–289. CRC Press, Boca Raton, FL.
20. Lockridge, O., Massey, V. & Sullivan, P.A. (1972) Mechanism of action of the flavoenzyme lactate oxidase. *J. Biol. Chem.* **247**, 8097–8106.
21. Porter, D.J.T., Voet, J.G. & Bright, H.J. (1977) Mechanistic features of the D-amino acid oxidase reaction studied by double stopped flow spectrophotometry. *J. Biol. Chem.* **252**, 4464–4473.
22. Schopfer, L.M., Massey, V. & Nishino, T. (1988) Rapid reaction studies on the reduction and oxidation of chicken liver xanthine dehydrogenase by the xanthine/urate and NAD/NADH couples. *J. Biol. Chem.* **263**, 13528–13538.
23. Smith, A.G. & Brooks, C.J.W. (1975) The mechanism of the isomerization of cholest-5-en-3-one to cholest-4-en-3-one by cholesterol oxidase. *Biochem. Soc. Trans.* **3**, 675–677.
24. Kamei, T., Takiguchi, Y., Suzuki, H., Matsuzaki, M. & Nakamura, S. (1978) Purification of 3-β-hydroxysteroid oxidase of *Streptomyces violascens* origin by affinity chromatography on cholesterol. *Chem. Pharm. Bull.* **26**, 2799–2804.
25. Inouye, Y., Taguchi, K., Fujii, A., Ishimaru, K., Nakamura, S. & Nomi, R. (1982) Purification and characterization of extracellular 3-β-hydroxysteroid oxidase produced by *Streptoverticillum cholesterolicum*. *Chem. Pharm. Bull.* **30**, 951–958.
26. Kass, I.J. & Sampson, N.S. (1995) The isomerization catalyzed by *Brevibacterium sterolicum* cholesterol oxidase proceeds stereospecifically with one base. *Biochem. Biophys. Res. Commun.* **206**, 688–693.
27. Martinek, K., Levashov, A.V., Klyachko, N., Khmelnitisky, Y.L. & Berezin, I.V. (1986). Micelle enzymology. *Eur. J. Biochem.* **155**, 453–468.
28. Dalziel, K. (1969) The interpretation of kinetic data for enzyme-catalyzed reactions involving three substrates. *Biochem. J.* **114**, 547–556.